

Elastic Moduli in Graphene Versus Hydrogen Coverage

E. Cadelano and L. Colombo

Abstract Through continuum elasticity we define a simulation protocol addressed to measure by a computational experiment the linear elastic moduli of hydrogenated graphene and we actually compute them by first principles. We argue that hydrogenation generally leads to a much smaller longitudinal extension upon loading than the one calculated for ideal graphene. Nevertheless, the corresponding Young modulus shows minor variations as function of coverage. Furthermore, we provide evidence that hydrogenation only marginally affects the Poisson ratio.

1 Introduction

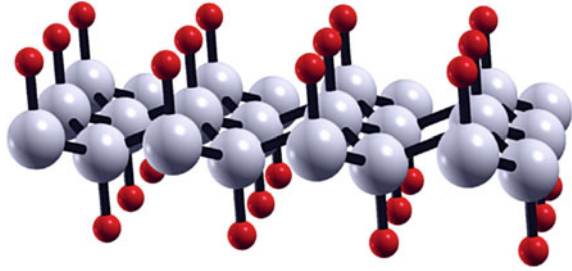
The hydrogenated form of graphene (also referred to as graphane) has been at first theoretically predicted by Sofo et al. [1] and Boukhvalov et al. [2], and eventually grown by Elias et al. [3]. More recently, a systematic study by Wen et al. [4] has proved that in fact there exist eight graphane isomers. They all correspond to covalently bonded hydrocarbons with a C:H ratio of 1. Interesting enough, four isomers have been found to be more stable than benzene, indeed an intriguing issue.

The attractive feature of graphane is that by variously decorating the graphene atomic scaffold with hydrogen atoms it is possible to generate a set of two dimensional materials with new physico-chemical properties. For instance, it has been calculated [1, 2] that graphane is an insulator, with an energy gap as large as ~ 6 eV [5], while

E. Cadelano (✉)
CNR-IOM (Unità SLACS), c/o Dipartimento di Fisica,
Cittadella Universitaria, Monserrato, I-09042 Cagliari, Italy
email: emiliano.cadelano@dsf.unica.it

L. Colombo
Dipartimento di Fisica dell'Università di Cagliari and CNR-IOM (Unità SLACS),
Cittadella Universitaria, Monserrato, I-09042 Cagliari, Italy
email: luciano.colombo@dsf.unica.it

Fig.1 Structure of ideal C-graphane with 100% hydrogen coverage. Hydrogen atoms are indicated by *red (dark)* spheres, while carbon ones by *gray (light)* spheres



graphene is a highly conductive semi-metal. In case the hydrogenated sample is disordered, the resulting electronic and phonon properties are yet again different [3].

As far as the elastic behavior is concerned, it has been proved that hydrogenation largely affects the elastic moduli as well. By blending together continuum elasticity theory and first principles calculations, Cadelano et al. [6] have determined the linear and non linear elastic moduli of three stable graphane isomers, namely : chair- (C-), boat-, and washboard-graphane. The resulting picture is very interesting; in particular, boat-graphene is found to have a small and negative Poisson ratio, while, due to the lack of isotropy, C-graphane admits both softening and hardening non linear hyperelasticity, depending on the direction of applied load.

Although full hydrogen coverage is possible and indeed proved to be stable in several non equivalent configurations [4], it is more likely that a typical experimental processing procedure generates samples with a C:H ratio larger than 1. In other words, we must admit that graphane could exist not only in a large variety of conformers, but also in several forms characterized by different stoichiometry.

In this work we present preliminary results about the variation of the linear elastic moduli of C-graphane (see Fig. 1), the most stable conformer [6], versus the hydrogen coverage. The goal is establish whether an incomplete sp^3 hybridization affects the elastic behavior and which is the trend (if any) of variation of the Young modulus and the Poisson ratio versus hybridization. A more extensive investigation addressed also to other graphane conformers will be published elsewhere.

2 Theory

Our multiscale approach benefits of continuum elasticity (used to define the deformation protocol aimed at determining the elastic energy density of the investigated systems) and first principles atomistic calculations (used to actually calculate such an energy density and the corresponding elastic moduli).

Atomistic calculations have been performed by Density Functional Theory (DFT) as implemented in the QUANTUM ESPRESSO package [7]. The exchange correlation potential was evaluated through the generalized gradient approximation (GGA) with the Perdew-Burke-Ernzerhof (PBE) parameterization [8], using Rabe Rappe

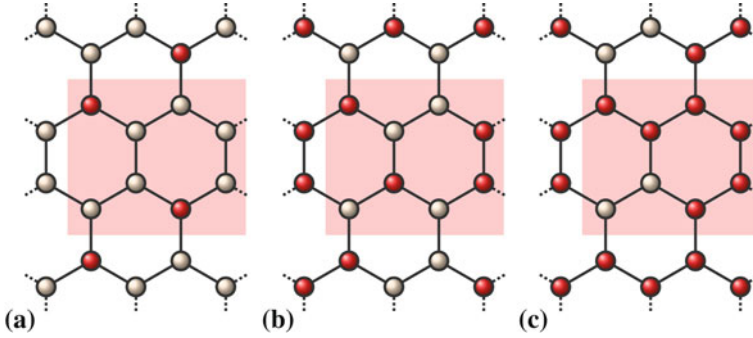


Fig. 2 Pictorial representations of different hydrogen motifs corresponding to a coverage of 25% (Panel a), 50% (Panel b), and 75% (Panel c). Hydrogen atoms are indicated by red (dark) circles, while hydrogen vacancies by gray (light) circles. Hydrogen atoms are randomly placed on the top or bottom of the graphene sheet. Shaded areas represent the simulation cell

Kaxiras Joannopoulos (RRKJ) ultrasoft pseudopotentials [9, 10]. A plane wave basis set with kinetic energy cutoff as high as 24 Ry was used and the Brillouin zone (BZ) has been sampled by means of a $(4 \times 4 \times 1)$ Monkhorst-Pack grid. The atomic positions of the investigated samples have been optimized by using damped dynamics and periodically-repeated simulation cells. Accordingly, the interactions between adjacent atomic sheets in the supercell geometry were hindered by a large spacing greater than 10 Å.

The elastic moduli of the structures under consideration have been obtained from the energy-vs-strain curves, corresponding to suitable deformations applied to samples with different hydrogen coverage, namely: 25, 50, and 75%, as shown in Fig. 2. The corresponding simulation cell (shaded area in Fig. 2) contained 8 carbon atoms and 2, 4, and 6 hydrogen atoms, respectively. As above said, they all correspond to C-graphane sheets with non ideal stoichiometry. For any possible coverage, several different geometries have been considered, by randomly placing hydrogen atoms according to different decoration motifs. This implies that all data below are obtained through configurational averages, a technical issue standing for the robustness of the present results.

As discussed in more detail in Ref. [6], for any deformation the magnitude of the strain is represented by a single parameter ζ . Thus, the strain-energy curves have been carefully generated by varying the magnitude of ζ in steps of 0.001 up to a maximum strain $\zeta_{max} = \pm 0.02$. All results have been confirmed by checking the stability of the estimated elastic moduli over several fitting ranges for each sample. The reliability of the above computational set up is proved by the estimated values for the Young modulus (E) and the Poisson ratio (ν) of graphene (corresponding to 0% of hydrogen coverage), respectively 349 Nm^{-1} and 0.15, which are in excellent agreement with recent literature [6, 11–14]. Similarly, our results for the same elastic moduli in C-graphane (corresponding to 100% of hydrogen coverage), respectively 219 Nm^{-1} and 0.21, agree with data reported in Ref. [6].

All the systems here investigated are elastically isotropic: C-graphane and graphene are so by crystallography; non stoichiometric C-graphane conformers with 25, 50 and 75% hydrogen coverage are so by assumption (which is indeed reasonable by only assuming that the hydrogen decoration in real samples is totally random). Accordingly, the elastic energy density (per unit of area) accumulated upon strain can be expressed as [15]

$$U = \frac{1}{2} \mathcal{C}_{11} (\varepsilon_{xx}^2 + \varepsilon_{yy}^2 + 2\varepsilon_{xy}^2) + \mathcal{C}_{12} (\varepsilon_{xx}\varepsilon_{yy} - \varepsilon_{xy}^2) \quad (1)$$

to the second order in the strain ε_{ij} , corresponding to the linear elasticity regime, where the x (y) label indicates the zigzag (armchair) direction in the hexagonal lattice of carbon atoms. In Eq. 1 we have explicitly made use of the linear elastic constants \mathcal{C}_{11} , \mathcal{C}_{22} , \mathcal{C}_{12} and \mathcal{C}_{44} by simply imposing the isotropy condition $\mathcal{C}_{11} = \mathcal{C}_{22}$ and the Cauchy relation $2\mathcal{C}_{44} = \mathcal{C}_{11} - \mathcal{C}_{12}$. Thus, the Young modulus E and Poisson ratio ν can be straightforwardly evaluated as $E = (\mathcal{C}_{11}^2 - \mathcal{C}_{12}^2)/\mathcal{C}_{11}$ and $\nu = \mathcal{C}_{12}/\mathcal{C}_{11}$, respectively. In the present formalism, the infinitesimal strain tensor $\hat{\varepsilon} = \frac{1}{2}(\vec{\nabla}\mathbf{u} + \vec{\nabla}\mathbf{u}^T)$ is represented by a symmetric matrix with elements $\varepsilon_{xx} = \frac{\partial u_x}{\partial x}$, $\varepsilon_{yy} = \frac{\partial u_y}{\partial y}$ and $\varepsilon_{xy} = \frac{1}{2} \left(\frac{\partial u_x}{\partial y} + \frac{\partial u_y}{\partial x} \right)$, where the functions $u_x(x, y)$ and $u_y(x, y)$ correspond to the planar displacement $\mathbf{u} = (u_x, u_y)$.

The constitutive in-plane stress-strain relations are straightforwardly derived from Eq. 1 through $\hat{T} = \partial U / \partial \hat{\varepsilon}$, where \hat{T} is the Cauchy stress tensor [16]. They are

$$\begin{cases} T_{xx} = \mathcal{C}_{11}\varepsilon_{xx} + \mathcal{C}_{12}\varepsilon_{yy} \\ T_{yy} = \mathcal{C}_{22}\varepsilon_{yy} + \mathcal{C}_{12}\varepsilon_{xx} \\ T_{xy} = 2\mathcal{C}_{44}\varepsilon_{xy} \end{cases} \quad (2)$$

This means that E and ν can be directly obtained from the linear elastic constants \mathcal{C}_{ij} , in turn computed through energy-vs-strain curves corresponding to suitable homogeneous in-plane deformations. Only two in-plane deformations should be in principle applied in order to obtain all the independent elastic constants, namely: (i) an uniaxial deformation along the zigzag (or armchair) direction; and (ii) an hydrostatic planar deformation. Nevertheless, for the validation of the isotropicity condition, two more in-plane deformations must be further applied: (iii) an axial deformation along the armchair (or zigzag) direction; and (iv) a shear deformation.

The strain tensors corresponding to applied deformations depend on the unique scalar strain parameter ζ [6, 14], so that the elastic energy of strained structures defined in Eq. 1 can be written as

$$U(\zeta) = U_0 + \frac{1}{2} U^{(2)} \zeta^2 + O(\zeta^3) \quad (3)$$

where U_0 is the energy of the unstrained configuration. Since the expansion coefficient $U^{(2)}$ is related to the elastic moduli, a straightforward fit of Eq. 3 has provided the full set of linear moduli for all structures. In Table 1 we report in detail the strain tensors describing the above deformations and the relationship between $U^{(2)}$ and the elastic constants \mathcal{C}_{ij} .

Table 1 Deformations and corresponding strain tensors applied to compute the elastic constants \mathcal{C}_{ij} , where ζ is the scalar strain parameter. The relation between such constants and the fitting term $U^{(2)}$ of Eq. 3 is reported as well. Deformations (i)–(ii) are enough to compute the independent set of elastic constants \mathcal{C}_{ij} , while the full set (i)–(iv) of deformations is needed to validate the assumed isotropicity condition

	Strain tensor	$U^{(2)}$ Isotropic structures
(1) Zigzag axial deformation	$\begin{pmatrix} \zeta & 0 \\ 0 & 0 \end{pmatrix}$	\mathcal{C}_{11}
(2) Hydrostatic planar deformation	$\begin{pmatrix} \zeta & 0 \\ 0 & \zeta \end{pmatrix}$	$2(\mathcal{C}_{11} + \mathcal{C}_{12})$
(3) Armchair axial deformation	$\begin{pmatrix} 0 & 0 \\ 0 & \zeta \end{pmatrix}$	$\mathcal{C}_{22} \equiv \mathcal{C}_{11}$
(4) Shear deformation	$\begin{pmatrix} 0 & \zeta \\ \zeta & 0 \end{pmatrix}$	$4\mathcal{C}_{44} \equiv 2(\mathcal{C}_{11} - \mathcal{C}_{12})$

Table 2 Independent elastic constants (units of Nm^{-1}) are shown for different values of the hydrogen coverage, between 0% (graphene) and 100% (C-graphane). The Young modulus E (units of Nm^{-1}), and the Poisson ratio ν are also shown

H-coverage	0% (graphene)	25%	50%	75%	100% (C-graphane)
\mathcal{C}_{11}	357 ± 7	267 ± 8	227 ± 12	258 ± 7	230 ± 10
\mathcal{C}_{12}	52 ± 11	51 ± 16	17 ± 27	10 ± 11	50 ± 20
E	349 ± 15	256 ± 10	230 ± 10	262 ± 10	219 ± 12
ν	0.15 ± 0.04	0.20 ± 0.03	0.10 ± 0.02	0.04 ± 0.04	0.21 ± 0.1

3 Results

The synopsis of the calculated elastic constants for all C-graphane samples, as well as graphene, is reported in Table 2, from which quite a few information can be extracted.

First of all, we remark that each hydrogenated conformer is characterized by a specific hydrogen arrangement and by a different buckling of the carbon sublattice. Moreover, due to the presence of unsaturated carbon atoms sites, during the relaxation we observed hydrogen jumps from the top to the bottom side of the graphene sheet (or vice versa), as well as in-plane hydrogen migration. An example is illustrated in Fig. 3. These features add further details to an already complex situation, inducing another source of disorder in the carbon sublattice mainly due to frustration between nearest neighbor hydrogens located at the same sheet side. Consequently, even where it is possible to distinguish between local graphene-like or graphane-like arrangements, we could hardly recognize as a chair-like structure the last one.

As a general feature emerging from Table 2, we state that the change in hybridization has largely reduced the property of longitudinal resistance upon extension, as described by the greatly reduced value of the Young modulus, about 30% lower with respect to ideal graphene. We argue that this is mainly due to the fact that sp^3

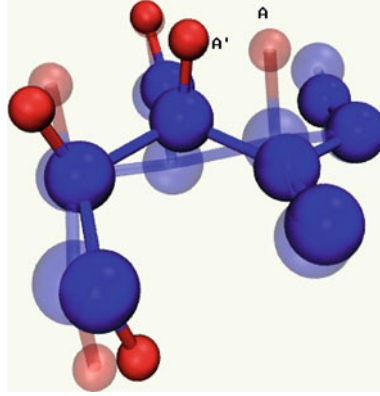


Fig.3 Pictorial representations of the input (transparent) and final (opaque) configuration of a C-graphene sample with the 50% hydrogen coverage. Hydrogen atoms are indicated by red (dark gray) small spheres and carbons by blue (black) ones. The hydrogen originally located at site A is displaced after relaxation in position labeled by A', leading to a more corrugated carbon sublattice

hybridization creates locally tetrahedral angles (involving 4 carbons and 1 hydrogen) which are easily distorted upon loading. In other words, softer tetrahedral deformations are observed, rather than bond stretching ones as in ideal graphene. In fact, the huge Young modulus of the flat sp^2 hexagonal lattice is due to the extraordinary strength of the carbon-carbon bonds. In this case, the applied in-plane stress (without bending) affects the lattice mainly through bond elongations; at variance, in hydrogenated samples deformations upon loading are basically accommodated by variations of the tetrahedral angles.

A key issue emerging from the above picture is that there exist more relaxation patterns upon loading than in pristine graphene. This ultimately reflects in a reduced Young modulus or, equivalently, to a floppy behavior upon elongation. We remark that, interesting enough, this feature occurs at any hydrogenated coverage: as the matter of fact, the reduction of the Young modulus value shows only a weak dependence on the actual hydrogen coverage, as shown in Fig. 4 (bottom). At variance, the top panel of Fig. 4 provides evidence that, within the accuracy of the present simulation set-up, the validity of the Poisson ratio is only marginally affected by hydrogenation.

Finally, we checked the assumed isotropy by computing explicitly the parameter $\mathcal{A} = 2\mathcal{C}_{44}/(\mathcal{C}_{11} - \mathcal{C}_{12})$, which should be 1 in such conditions. Indeed our results display an \mathcal{A} value as large as 1.0 ± 0.2 , which confirms that isotropic elasticity is verified within about 10%.

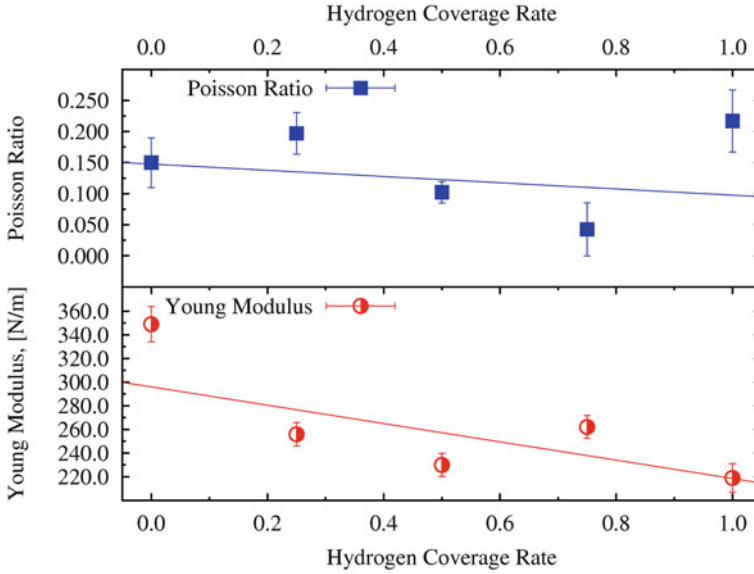


Fig. 4 Elastic moduli are shown as function of the hydrogen coverage. The *straight lines* correspond to a linear regression

4 Conclusions

We have presented and discussed preliminary first principles calculations predict that the elastic behavior of graphene is largely affected by hydrogen absorption, but it shows minor variations as function of the coverage. In particular, while the Young modulus is greatly reduced upon hydrogenation, the Poisson ratio is nearly unaffected. An incomplete coverage generates a large configurational disorder in the hydrogen sublattice, leading to a larger corrugation with respect to highly-symmetric C-graphane. Indeed, such a corrugation of the carbon sublattice is a key feature affecting the overall elastic behavior.

Acknowledgements We acknowledge financial support by Regional Government of Sardinia under the project “Ricerca di Base” titled “Modellizzazione Multiscala della Meccanica dei Materiali Complessi” (RAS-M4C).

References

1. Sofo, J.O., Chaudhari, A.S., Barber, G.D.: Phys. Rev. B **75**, 153401 (2007)
2. Boukhvalov, D.W., Katsnelson, M.I., Lichtenstein, A.I.: Phys. Rev. B **77**, 035427 (2008)

3. Elias, D.C., Nair, R.R., Mohiuddin, T.M.G., Morozov, S.V., Blake, P., Halsall, M.P., Ferrari, A.C., Boukhvalov, D.W., Katsnelson, M.I., Geim, A.K., Novoselov, K.S.: *Science* **323**, 610 (2009)
4. Wen, X.-D., Hand, L., Labet, V., Yang, T., Hoffmann, R., Ashcroft, N.W., Oganov, A.R., Lyakhov, A.O.: *Proc. Nat. Acad. Sci. U.S.A.* **108**, 6833 (2011)
5. Lebègue, S., Klintenberg, M., Eriksson, O., Katsnelson, M.I.: *Phys. Rev. B* **79**, 245117 (2009)
6. Cadelano, E., Palla, P.L., Giordano, S., Colombo, L.: *Phys. Rev. B* **23**, 235414 (2010)
7. Giannozzi, P., Baroni, S., Bonini, N., Calandra, M., Car, R., Cavazzoni, C., Ceresoli, D., Chiarotti, G.L., Cococcioni, M., Dabol, I., Dal Corso, A., de Gironcoli, S., Fabris, S., Fratesi, G., Gebauer, R., Gerstmann, U., Gougoussis, C., Kokalj, A., Lazzeri, M., Martin-Samos, L., Marzari, N., Mauri, F., Mazzarello, R., Paolini, S., Pasquarello, A., Paulatto, L., Sbraccia, C., Scandolo, S., Sclauzero, G., Seitsonen, A.P., Smogunov, A., Umari, P., Wentzcovitch, R.M.: *J. Phys.: Condens. Matter* **21**, 395502 (2009)
8. Perdew, J.P., Burke, K., Ernzerhof, M.: *Phys. Rev. Lett.* **77**, 1396(E) (1997)
9. Rappe, A.M., Rabe, K.M., Kaxiras, E., Joannopoulos, J.D.: *Phys. Rev. B* **41**, 1227 (1990)
10. Mounet, N., Marzari, N.: *Phys. Rev. B* **71**, 205214 (2005)
11. Kudin, K.N., Scuseria, E., Yakobson, B.I.: *Phys. Rev. B* **64**, 235406 (2001)
12. Gui, G., Li, J., Zhong, J.: *Phys. Rev. B* **78**, 075435 (2008)
13. Liu, F., Ming, P., Li, J.: *Phys. Rev. B* **76**, 064120 (2007)
14. Cadelano, E., Palla, P.L., Giordano, S., Colombo, L.: *Phys. Rev. Lett.* **102**, 235502 (2009) (and references therein).
15. Huntington, H.B.: *The Elastic Constants of Crystals*. Academic Press, New York (1958)
16. Landau, L.D., Lifschitz, E.M.: *Theory of Elasticity*. Butterworth Heinemann, Oxford (1986)

GraphITA 2011

Selected papers from the Workshop on Fundamentals
and Applications of Graphene

Ottaviano, L.; Morandi, V. (Eds.)

2012, X, 231 p., Hardcover

ISBN: 978-3-642-20643-6